Eighth Hungarian Conference on Computer Graphics and Geometry, Budapest, 2016

Direct Parametric Reconstruction for Dynamic PET

László Szirmay-Kalos and Ágota Kacsó

Budapest University of Technology and Economics (e-mail: szirmay@iit.bme.hu)

Abstract

This paper proposes a scalable dynamic PET reconstruction approach for GPUs. In dynamic PET reconstruction the space-time activity function needs to be recovered from measurements. Based on the maximum likelihood principle, the reconstruction looks for the space-time functions that maximize the probability of the actual measurements. The number of spatial basis functions is in the range of a hundred million, the number of frames of the discretized temporal description exceeds a hundred, while the number of events can exceed billions. To reduce the storage requirements and the computation time, we propose a factorization approach that decomposes the iterative solutions to a sequence of sub-iterations of elementary steps, each can be executed in parallel without communication between threads, allowing exchange of information just between the elementary steps.

1. Introduction

In dynamic Positron Emission Tomography (PET), we focus on the dynamic nature of biological processes, like accumulation and emptying drugs in certain organs. Such studies are essential in pharmaceutical research. Dynamic tomography reconstructs a space-time density $x(\vec{v},t)$, from which kinetic rate parameters are obtained. Generally, we assume that the time activity of a point $\vec{v}$ can be expressed by a common *kinetic model* $F(\theta(\vec{v}),t)$, where spatial dependent properties are encoded in a low dimensional vector of parameters θ. Such models can be defined based on the mathematical description of the biological/chemimal processes or on compartment analysis.

Time activity $F(\theta,t)$ depends on the concentration $C(\theta,t)$ of the radiotracer and on the known decay constant λ of the radiotracer:

$$F(\theta,t) = C(\theta,t)\exp(-\lambda t).$$

In this paper we use the *two-tissue-compartment* model that is based on the solution of differential equations describing material exchange between compartments. Thus the concentration is searched in the form of a linear combination of the convolutions of an exponential with unknown parameter and the known *blood input function* $C_p(t)$ that describes the radiotracer concentration in the blood from where diffusion can start:

$$C(\theta,t) = a_1 \cdot \alpha_1 \exp(-\alpha_1 t) * C_p(t) + a_2 \cdot \alpha_2 \exp(-\alpha_2 t) * C_p(t), \quad (1)$$

where every voxel is associated with four unknown parameters $\theta = (a_1, a_2, \alpha_1, \alpha 2)$. Note that it would be possible to consider $a_1 \cdot \alpha_1$ as a free parameter instead of a_1, but the form of Equation 1 is better since it makes the parameters more independent as the integral of the activity curve is mainly determined by a_1 and a_2 and less affected by exponents α_1, α_2.

If the reconstruction and kinetic parameter estimation are separated and executed after each other, the approach is indirect. In a *direct method*, reconstruction and parameter estimation are merged into the same process, and the temporal functions are always computed from the kinetic parameters. Direct reconstruction can be considered as a regularization in the time domain since we impose the requirement that the resulting temporal functions must belong to the class represented by the kinetic model.

Using the space-time density, the expected number of radioactive decay, i.e. number of positrons generated in differential volume dv and in differential time dt is $x(\vec{v},t)$dvdt. The positron emitted at a decay is drifted in the volume and soon annihilates with an electron, when two oppositely directed gamma-photons are born, which might be detected by the tomograph. A PET/CT system collects the *events* of simultaneous photon incidents in detector pairs. An event is a composition of the identification of the detector pair, also called *Line Of Response* or *LOR* and its time of occurrence. *List mode* reconstructions process this row data. For more efficient processing, the measurement time is decomposed

into finite time intervals, called frames $\Delta t_1, \ldots, \Delta t_{N_T}$ with interval centers $t_1, \ldots, t_T$, and events are binned in frames. We denote the number of events in LOR L and frame T by $y_{L,T}$. This decomposition reduces the time complexity from the number of events to the number of frames N_T, but loses the information of the actual time of the events within a frame.

The spatial variation of the activity is typically defined in a finite-element form [14, 2, 3, 4, 21, 12]. In the simplest case, the domain decomposed to voxels and in each voxel the points are assumed to have the same temporal activity function. Combining the spatial variation with the temporal function defined by the kinetic model, the spatio-temporal activity function is:

$$x(\vec{v},t) = \sum_V F(\theta_V, t) b_V(\vec{v})$$

where $b_V(\vec{v})$ is the spatial basis function of voxel V. For example, in piece-wise constant spatial reconstruction, b_V is a positive constant if $\vec{v}$ is in voxel V and zero otherwise. The reconstructed function can be visualized with many different algorithms[1].

2. Dynamic PET reconstruction

The correspondence between positron generation and gamma photon detection is established by *scanner sensitivity* $\mathcal{T}(\vec{v} \to L)$ that expresses the probability of generating an event in LOR L given that a positron is emitted in point $\vec{v}$ of volume $\mathcal{V}$. We assume that the scanner sensitivity is constant in time and is independent of the current activity. The scanner sensitivity is a high-dimensional integral of variables unambiguously defining the path of particles from positron emission point $\vec{v}$ to the detector electronics.

The event rate $\lambda_L(t)$ in LOR L at time t is the sum of the contributions of all points in the volume at this time (note that we ignore the time elapsed between positron generation and gamma photon detection):

$$\lambda_L(t) = \int_{\mathcal{V}} x(\vec{v},t)\mathcal{T}(\vec{v} \to L)\mathrm{d}v = \sum_{V=1}^{N_V} \mathbf{A}_{LV} F(\theta_V, t)$$

where *system matrix*

$$\mathbf{A}_{L,V} = \int_{\mathcal{V}} \mathcal{T}(\vec{v} \to L) b_V(\vec{v})\mathrm{d}v$$

defines the correspondence between voxel V and LOR L.

During iterative *Expectation Maximization* (ML-EM) reconstruction [13], unknown coefficients are found to maximize the probability of the actually measured data. The measured number of hits in LOR L in time interval Δt_T follows a Poisson distribution of expectation $\lambda_L(t_T)\Delta t_T$:

$$P\{y_{L,T}\} = \frac{(\lambda_L(t_T)\Delta t_T)^{y_{L,T}}}{y_{L,T}!} \cdot e^{-\lambda_L(t_T)\Delta t_T}.$$

Because of the statistical independence of different LORs and different frames, the combined probability considering all LORs and all frames is the product of elementary probabilities:

$$\mathcal{L} = \prod_{T=1}^{N_T} \prod_{L=1}^{N_L} \frac{(\lambda_L(t_T)\Delta t_T)^{y_{L,T}}}{y_{L,T}!} \cdot e^{-\lambda_L(t_T)\Delta t_T}.$$

The log-likelihood function is:

$$\log \mathcal{L} = \sum_{T=1}^{N_T} \sum_{L=1}^{N_L} \log\left(\frac{(\lambda_L(t_T)\Delta t_T)^{y_{L,T}}}{y_{L,T}!} e^{-\lambda_L(t_T)\Delta t_T} \right) =$$

$$\sum_{L=1}^{N_L} \left(\sum_{T=1}^{N_T} y_{L,T} \log \lambda_L(t_T) - \sum_{T=1}^{N_T} \lambda_L(t_T)\Delta t_T \right) + C,$$

where

$$C = \sum_{T=1}^{N_T} \sum_{L=1}^{N_L} y_{L,T} \log(\Delta t_T) - \log(y_{L,T}!)$$

is a constant that depends on the measurement intervals and hit numbers but is independent of activity function λ, which in turn depends on unknown parameters $\theta_{V,P}$.

According to the concept of maximum-likelihood reconstruction, unknown parameters are found to maximize this likelihood:

$$\theta = \arg\max \sum_L \sum_T \left(y_{L,T} \log \lambda_L(t_T) - \lambda_L(t_T)\Delta t_T \right). \qquad (2)$$

The optimization problem has very high computational complexity. The number of free variables, i.e. the dimension of the search space is $N_P \times N_V$, the target is a sum of $N_L \times N_T$ terms, and both of them can be over a billion. This means that the search method should be carefully designed and high performance computation platforms should be exploited.

3. GPU implementation issues

In order to exploit the computational power of GPUs, we have to cope with the quasi-SIMD architecture of current GPUs and tailor the solution algorithm accordingly [17, 18]. By quasi-SIMD architecture we mean that the GPU is able to execute the same program in parallel on a large data, but its performance degrades when different computational threads visit different branches of the control flow. Ideally, the control path of threads must be identical for all input data. Adding more parallel processors results in linear speed up if threads execute the program independently, i.e. communication and synchronization do not destroy the efficiency.

When we have to compute a vector of output data from a vector of input data, the "many to many" computation can be organized in two different ways. We can take known values one-by-one, obtain the contribution of a single known value to all of the unknowns, and accumulate the contributions as different known values are visited. We call this scheme *shooting*. The orthogonal approach would take unknown values (i.e. equations) one-by-one, and obtain the contribution

of all known values to this particular unknown value. This approach is called *gathering*. We emphasize that the distinction of these cases might be just the order of loops in a CPU implementation, but is a crucial design decision when the algorithm is run on the GPU since it defines which loop is executed in parallel on the shader processors. GPUs and in general parallel algorithms favor gathering since it computes a single result from the available data, which can be written out without communicating between and synchronizing of the computational threads.

4. Previous work

The state of the art and previous work on direct estimation of kinetic parametric images for dynamic PET are surveyed in review article [7].

If the kinetic model is a linear function of non-negative parameters, then the classical ML-EM scheme can be extended to find all parameters [10]. Biologically plausible kinetic models often depend on their parameters non-linearly, rendering the classical ML-EM approach not applicable anymore. A first approach aiming at the reconstruction of parameters of the two-tissue-compartment model for each voxel rather than only for a few ROIs searched the maximum of a penalized likelihood with the parametric iterative coordinate descent algorithm [8]. The one-compartment model was considered in [23]. Wang et al. [22] proposed the application of optimization transfer to find the optimum for general kinetic models, which locally approximated the objective function of the optimization. This method alternates independent reconstructions of the frames and model fitting in iteration steps.

5. The proposed method

The reconstruction means the solution of the optimization problem of Equation 2. The likelihood has an extremum where all partial derivatives are zero:

$$\frac{\partial \log \mathcal{L}}{\partial \theta_{V,P}} = 0. \tag{3}$$

Computing the partial derivatives, we obtain

$$\frac{\partial \log \mathcal{L}}{\partial \theta_{V,P}} = \sum_T \left.\frac{\partial F}{\partial \theta_{V,P}}\right|_{t_T} \sum_L \mathbf{A}_{L,V} \left(\frac{y_{L,T}}{\sum_{V'} \mathbf{A}_{L,V'} F(\theta_{V'}, t_T)} - \Delta t_T \right). \tag{4}$$

for $V = 1, 2, \ldots, N_V$ and $P = 1, \ldots, N_P$. Thus, we have $N_V \times N_P$ equations, each containing N_T terms that depend on unknown parameters of all voxels $\theta_{V,P}$, and the computation of each equation requires the consideration of all LORs L for which $\mathbf{A}_{L,V}$ is not zero. Note that accurate reconstruction requires the computation of scattered particle paths as well, which makes system matrix $\mathbf{A}$ not sparse.

The range of N_V and N_L is typically several hundred millions, N_T is typically in the order of a hundred, and N_P is less than 10 since we wish to describe a time function with a few parameters. Concerning the evaluation and the solution of this equation on massively parallel architectures, the process should be decomposed to phases where computational threads are assigned either to voxels or LORs since their numbers are high enough to utilize all parallel processors of a GPU, while we should avoid storage complexity where any product of factors N_L, N_V, and N_T shows up.

To achieve this goal, the computation of the derivative of the likelihood function is decomposed to steps that can be executed by the GPU, and its iterative solution is decomposed to sub-iterations (Figure 1). Let us first consider the evaluation of the derivative of the log-likelihood function.

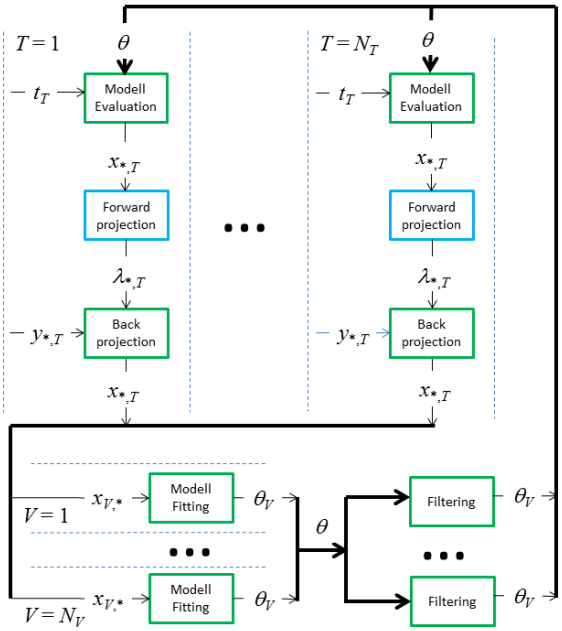

Figure 1: *System overview*

5.1. Forward projection in frame T

Note that the factor in parentheses of Equation 4 describes a static forward projection and back projection in frame T. Indeed, in frame T, the event rate of radioactive decays in voxel V is $F(\theta_V, t_T)$, which is forward projected as

$$\lambda_{L,T} = \sum_{V'} \mathbf{A}_{L,V'} F(\theta_{V'}, t_T)$$

to get the event rate of hits in LOR L in frame T. A gathering type approach is obtained if computational threads are assigned to LORs and each thread computes the event rate for a single LOR L at a fixed frame T [16, 15].

With these notations, the partial derivatives become

$$\frac{\partial \log \mathcal{L}}{\partial \theta_{V,P}} = \sum_T \left.\frac{\partial F}{\partial \theta_{V,P}}\right|_{t_T} \left(\sum_L \mathbf{A}_{L,V} \frac{y_{L,T}}{\lambda_{L,T}} - \sum_L \mathbf{A}_{L,V} \Delta t_T \right). \tag{5}$$

5.2. Back projection in frame T

A static back projection would obtain a new estimate of the activity as

$$x_{V,T} = F(\theta_V, t_T) \cdot \frac{\sum_L \mathbf{A}_{L,V} \frac{y_{L,T}}{\lambda_{L,T}}}{\sum_L \mathbf{A}_{L,V}}.$$

Note that this step is a classical ML-EM step, where a gathering algorithm assigns computational threads to voxels and each thread computes a single value $x_{V,T}$ [16, 15]. From this equation, we can express the first term in parentheses of Equation 5:

$$\sum_L \mathbf{A}_{L,V} \frac{y_{L,T}}{\lambda_{L,T}} = \left(\sum_L \mathbf{A}_{L,V} \right) \frac{x_{V,T}}{F(\theta_V, t_T)}.$$

Thus the new form of the derivative of the likelihood is:

$$\frac{\partial \log \mathcal{L}}{\partial \theta_{V,P}} = \sum_T \left. \frac{\partial F}{\partial \theta_{V,P}} \right|_{t_T} \left(\sum_L \mathbf{A}_{L,V} \right) \left(\frac{x_{V,T}}{F(\theta_V, t_T)} - \Delta t_T \right). \tag{6}$$

5.3. Root finding

In Equation 7 the partial derivatives are equal to zero. Dividing both sides by the sensitivity of the voxel, i.e. by $\sum_L \mathbf{A}_{L,V}$, we get an equivalent requirement for the extremum of the likelihood

$$\sum_T \left. \frac{\partial F}{\partial \theta_{V,P}} \right|_{t_T} \left(\frac{x_{V,T}(\theta)}{F(\theta_V, t_T)} - \Delta t_T \right) = 0. \tag{7}$$

In this equation F depends on unknown parameter vector of the given voxel θ_V, while $x_{V,T}$ depends on the parameter vectors of all voxels. Additionally, $x_{V,T}$ is the only factor that is affected by other voxels and the elements of the system matrix. Thus, if $x_{V,T}$ were known, then the computation could be decoupled for different voxels, where a system of equations of N_P unknowns needs to be solved. In this way, forward/backward projection can be separated from the parameter fitting, thus the complexity of the algorithm will be the sum of the complexities of the two steps and not their product.

The non-linear equation is solved iteratively, where a step involves a subiteration for the execution of a simpler non-linear equation for $\theta_V^{(n+1)}$:

$$\sum_T \left. \frac{\partial F(\theta_V^{(n+1)})}{\partial \theta_{V,P}} \right|_{t_T} \left(\frac{x_{V,T}(\theta^{(n)})}{F(\theta_V^{(n+1)}, t_T)} - \Delta t_T \right) = 0. \tag{8}$$

If this iteration scheme is convergent, then it obviously converges to the real solution. The left side of this equation is a function of unknown parameter $\theta_V^{(n+1)}$, which is denoted by $\xi(\theta_V^{(n+1)})$

Assuming that $x_{V,T}$ is constant, Equation 8 describes just a single voxel, and can thus be solved independently for all voxels. The solution of this equation is a set of parameters for this particular voxels, which define a time activity curve $F(\theta_V, t)$ that fits to $x_{V,T}$. Assigning computational threads of the GPU to voxels, this fitting is done in parallel for all voxels. The fitting itself is iterative. In each iteration step, $\theta^{(n+1),(k+1)})$ should be expressed from $\theta^{(n+1),(k)})$, for which, we use the Iteractive Coordinate Descent algorithm, i.e. apply the Newton-Raphson update for each coordinate P circularly:

$$\theta_{V,P}^{(n+1),(k+1)} = \theta_{V,P}^{(n+1),(k)} - \frac{\xi(\theta_V^{(n+1),(k)})}{\xi'(\theta_V^{(n+1),(k)})}.$$

5.4. Spatial filtering of parameters

There are various options to regularize the solution, which is essential in the case of inverse problems. One option is the modification of the optimization target in Equation 2 by a regularization term that penalizes unacceptable solutions, where, for example, the spatial or temporal variation is too high. Due to the computation of the partial derivatives, this approach would add the derivative of the regularization term to Equation 8. In this paper, we use another option, proposed by the *method of sieves*. In this approach, the optimization target is not modified, but the iterated approximation is filtered in each iteration step. The objective of filtering is to find an acceptable solution that is close to the solution proposed by the iteration. Mathematically, this approach projects the current estimate into the subspace of acceptable solutions in each iteration. Filtering can also exploit anatomic information gathered by a CT or an MR [19].

5.5. System overview

Putting the discussed steps together, we obtain the system of Figure 1. The pseudo-code of the reconstruction is as follows:

for $n = 1$ **to** $n_{\max}$ **do**
  for $T = 1$ **to** N_T **do**
    foreach LOR L **in parallel** *// forward projection*
      $\lambda_{L,T} = \sum_{V'} \mathbf{A}_{L,V'} F(\theta_{V'}^{(n)}, t_T)$
    foreach voxel V **in parallel** *// back projection*
      $x_{V,T} = F(\theta_V^{(n)}, t_T) \cdot \frac{\sum_L \mathbf{A}_{L,V} \frac{y_{L,T}}{\lambda_{L,T}}}{\sum_L \mathbf{A}_{L,V}}$
  endfor
  foreach voxel V **in parallel** *// curve fitting*
    $\theta_V^{(n+1)} = \text{Solve}\left\{ \sum_T \left. \frac{\partial F}{\partial \theta_{V,P}} \right|_{t_T} \left(\frac{x_{V,T}(\theta^{(n)})}{F(\theta_V^{(n+1)}, t_T)} - \Delta t_T \right) = 0 \right\}$
  foreach voxel V **in parallel** *// spatial regularization*
    $\theta_V^{(n+1)} = \text{Filter}(\theta, \text{anatomy})$
endfor

6. Results

To examine the proposed method, we use a 2D model [16] where $N_L = 2115$ and $N_V = 1024$ (Fig. 2) and reconstruct

the activity curves of a 2D brain model. For this model, the system matrix can be precisely computed.

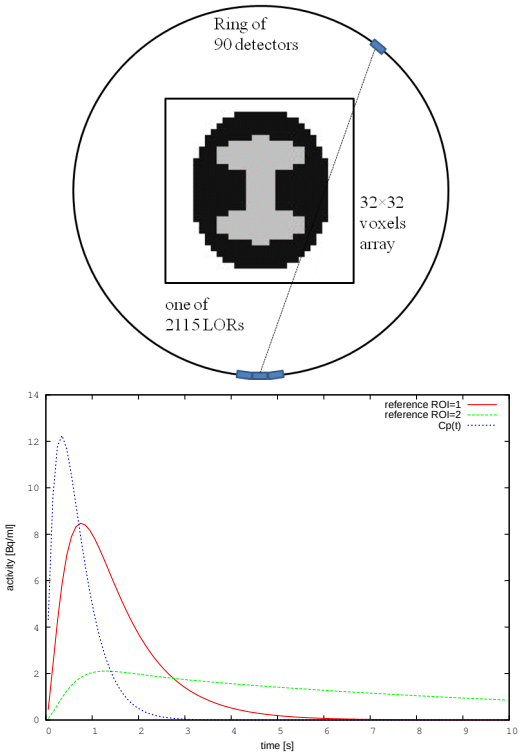

Figure 2: *2D tomograph model: The detector ring contains 90 detector crystals and each of them is of size 2.2 in voxel units and participates in 47 LORs connecting this crystal to crystals being in the opposite half circle, thus the total number of LORs is* $90 \times 47/2 = 2115$. *The voxel array to be reconstructed is in the middle of the ring and has* 32×32 *resolution, i.e. 1024 voxels. The lower image shows the blood input function and the simulated time activity curves in the gray matter (ROI 2) and white matter (ROI 1) of the brain.*

The two-tissue-compartment model is applied both for the generation of measured hits in LORs and for the reconstruction of temporal activity function in each voxel. We decomposed 10 time units to different number of time frames (50, 100 and 200). In all the cases 10 iterations are executed.

Regarding the effect of the frame numbers on the quality of reconstruction, more frames can show finer dynamic changes, but it is also obvious that as the frame number is increasing the total number of hits in a given time frame is decreasing (Figure 3), thus reducing the quality of reconstruction. As a consequence the standard deviation of the voxel activities belonging to same region of interest (ROI) is increasing. However this effect can be eliminated using regularization (Figure 4).

The effect of the total activity on the quality of reconstruction is examined similarly. As the total activity is increasing, the number of hits in LORs is increasing (Figure 5) and the reconstruction gets more accurate (Figure 6). We also compared the parametric and non parametric reconstruction. It can be seen that in both cases the application of regularization highly improved the quality of reconstruction, but the parametric reconstruction proves to be more efficient (Figure 6).

In order to decrease the initial total activity error, at initialize a frame with the already iterated estimation of the previous frame. This is certainly a better initial guess than the original initial constant activity values, which results in a better error curve (Figure 7).

Figure 8 shows examples of reconstructed spatial activities at time $t = 1$ in case of several total activities and for all the discussed reconstruction strategies.

7. Conclusions

In this paper we investigated the problem of dynamic, parametric PET reconstruction when the total activity in voxels needs to be reconstructed as a function of time. We have proposed a solution method where phases are GPU friendly, i.e. can be decomposed to many parallel threads and have moderate complexity characteristics. The method has been examined with a 2D example, but we are also working on its fully 3D extension.

Acknowledgement

This work has been supported by OTKA K–104476 and VKSZ-14 PET/MRI 7T projects.

References

1. B. Csébfalvi. *Interactive Volume-Rendering Techniques for Medical Data Visualization*. PhD thesis, Technische Universität Wien, Institut für Computergraphik und Algorithmen, 2001. http://www.cg.tuwien.ac.at/research/theses/.

2. B. Csébfalvi. An evaluation of prefiltered reconstruction schemes for volume rendering. *IEEE Transactions on Visualization and Computer Graphics*, 14(2):289–301, 2008.

3. B. Csébfalvi. An evaluation of prefiltered B-spline reconstruction for quasi-interpolation on the body-centered cubic lattice. *IEEE Transactions on Visualization and Computer Graphics*, 16(3):499–512, 2010.

4. B. Csébfalvi. Cosine-weighted B-spline interpolation: A fast and high-quality reconstruction scheme for the body-centered cubic lattice. *IEEE Transactions on Visualization and Computer Graphics*, 19(9):1455–1466, 2013.

5. Balázs Csébfalvi. Prefiltered gaussian reconstruction for high-quality rendering of volumetric data sampled on a body-centered cubic grid. In *VIS '05: Visualization, 2005*, pages 311–318. IEEE Computer Society, 2005.

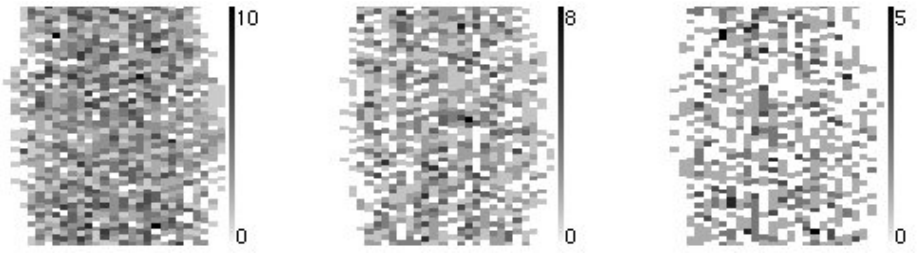

50 frames 100 frames 200 frames

Figure 3: *The number of hits in LORs at $t = 1$, when the total number of hits is 78655.*

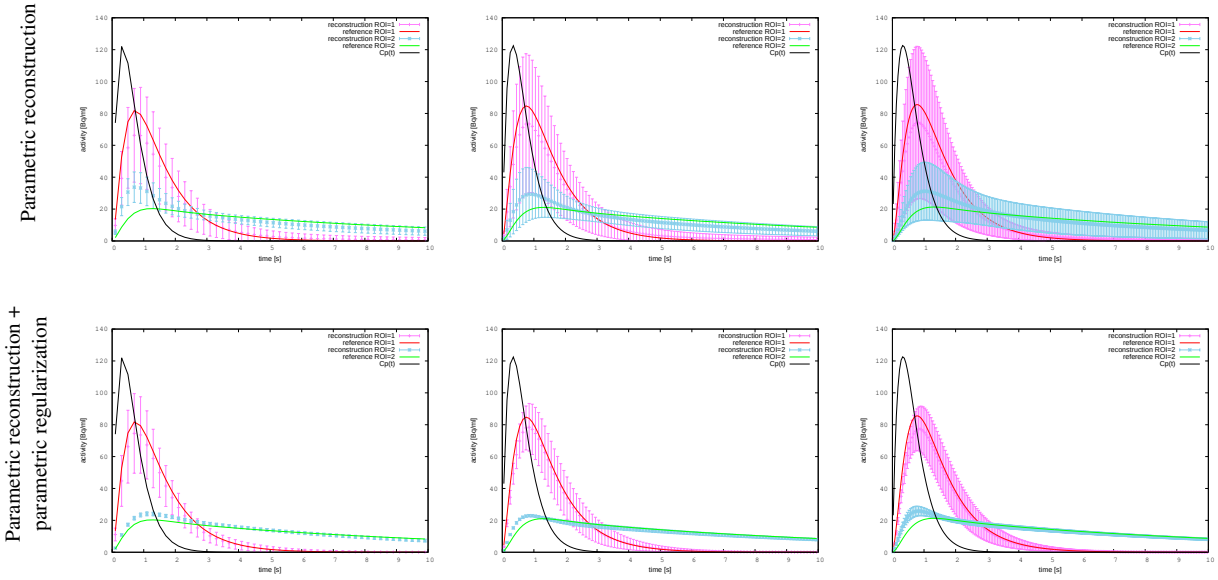

50 frames 100 frames 200 frames

Figure 4: *Time activity functions of voxels in different ROIs. The average and the standard deviation are depicted.*

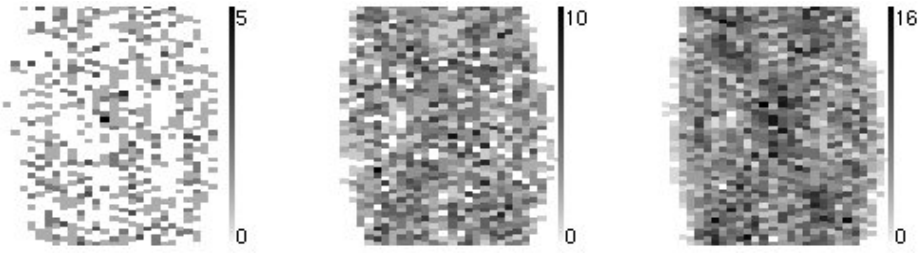

15736 hits 78655 hits 157185 hits

Figure 5: *The number of hits in LORs at $t = 1$, 100 frames are defined.*

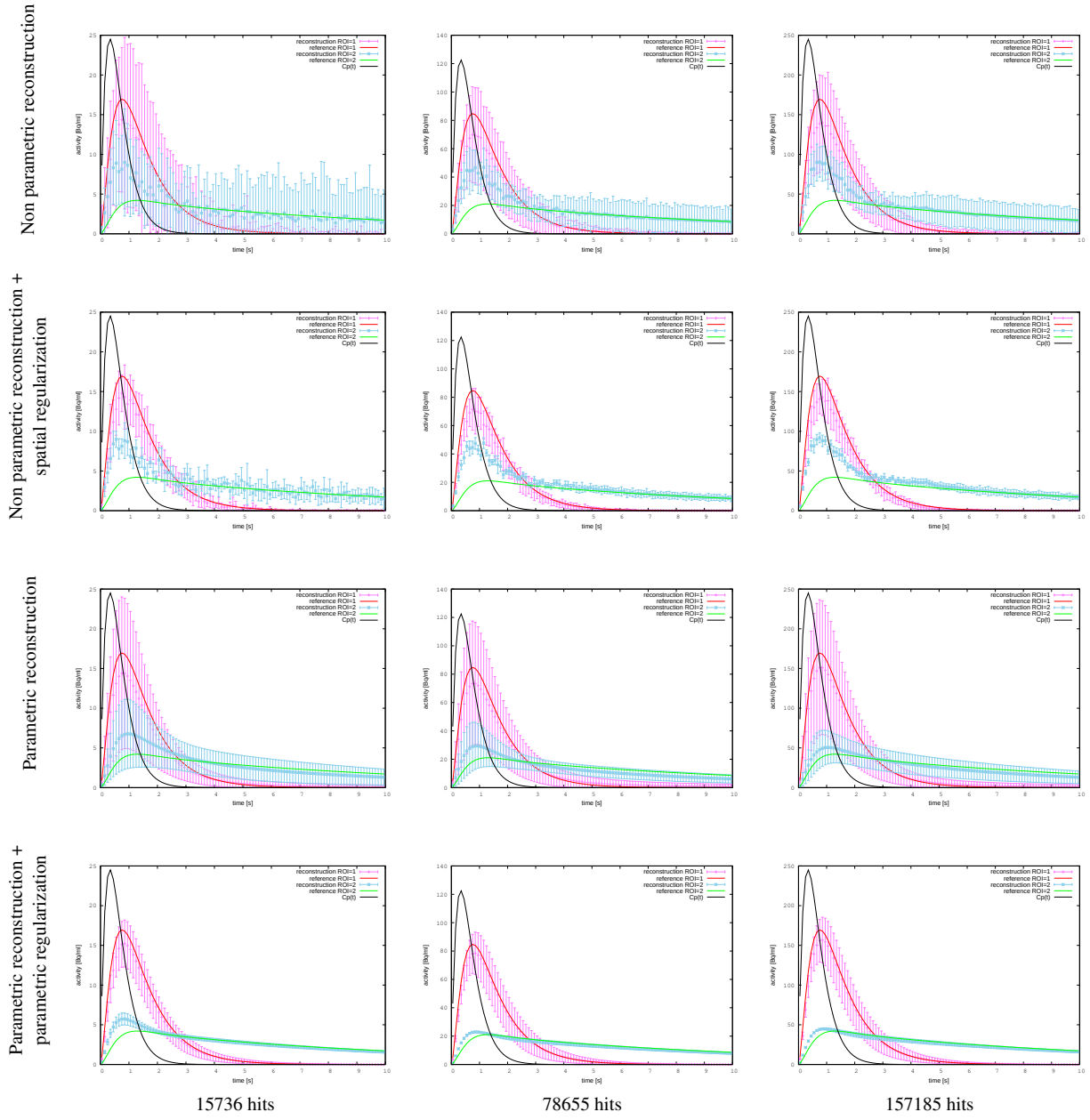

Figure 6: *Time activity functions of voxels in different ROIs. The average and the standard deviation are depicted.*

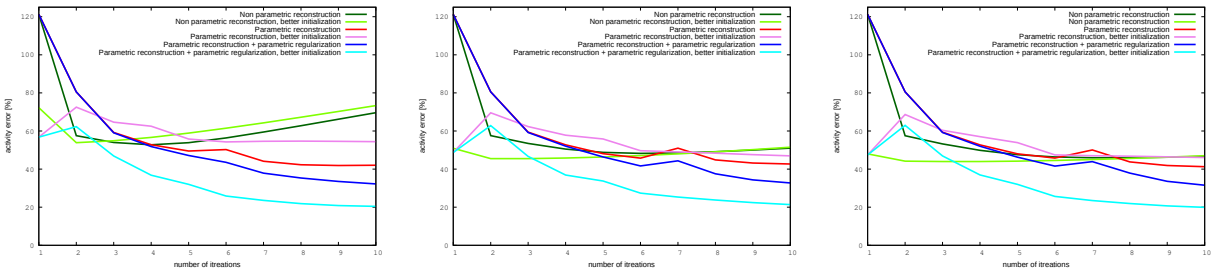

15736 hits 78655 hits 157185 hits

Figure 7: *Error of the time activity functions.*

6. Balázs Csébfalvi, Lukas Mroz, Helwig Hauser, Andreas König, and Eduard Gröller. Fast visualization of object contours by non-photorealistic volume rendering. *Computer Graphics Forum*, 20(3):452–460, 2001.

7. M.E. Kamasak, C.A. Bouman, E.D. Morris, and K. Sauer. Direct reconstruction of kinetic parameter images from dynamic pet data. *Medical Imaging, IEEE Transactions on*, 24(5):636–650, May 2005.

8. M. Magdics and et al. Performance Evaluation of Scatter Modeling of the GPU-based "Tera-Tomo" 3D PET Reconstruction. In *IEEE Nuclear Science Symposium and Medical Imaging*, pages 4086–4088, 2011.

9. J. Matthews, D. Bailey, P. Price, and V. Cunningham. The direct calculation of parametric images from dynamic PET data using maximum-likelihood iterative reconstruction. *Physics in Medicine and Biology*, 42:1155–1173, June 1997.

10. László Papp, Gábor Jakab, Balázs Tóth, and László Szirmay-Kalos. Adaptive bilateral filtering for PET. In *IEEE Nuclear science symposium and medical imaging conference*, MIC'14, pages M18–104, 2014.

11. G. Rácz and B. Csébfalvi. Tomographic reconstruction on the body-centered cubic lattice. In *Proceedings of Spring Conference on Computer Graphics (SCCG)*, 2015.

12. L. Shepp and Y. Vardi. Maximum likelihood reconstruction for emission tomography. *IEEE Trans. Med. Imaging*, 1:113–122, 1982.

13. L. Szirmay-Kalos. *Monte-Carlo Methods in Global Illumination — Photo-realistic Rendering with Randomization*. VDM, Verlag Dr. Müller, Saarbrücken, 2008.

14. L. Szirmay-Kalos, M. Magdics, and B. Tóth. Multiple importance sampling for PET. *IEEE Trans Med Imaging*, 33(4):970–978, 2014.

15. L. Szirmay-Kalos, M. Magdics, B. Tóth, and T. Bükki. Averaging and Metropolis iterations for positron emission tomography. *IEEE Trans Med Imaging*, 32(3):589–600, 2013.

16. L. Szirmay-Kalos and L. Szécsi. General purpose computing on graphics processing units. In A. Iványi, editor, *Algorithms of Informatics*, pages 1451–1495. MondArt Kiadó, Budapest, 2010. http://sirkan.iit.bme.hu/szirmay/gpgpu.pdf.

17. L. Szirmay-Kalos, L. Szécsi, and M. Sbert. *GPU-Based Techniques for Global Illumination Effects*. Morgan and Claypool Publishers, San Rafael, USA, 2008.

18. László Szirmay-Kalos, Milán Magdics, and Balázs Tóth. Volume enhancement with externally controlled anisotropic diffusion. *The Visual Computer*, pages 1–12, 2016.

19. Márton Tóth and Balázs Csébfalvi. Shape transformation of multidimensional density functions using distribution interpolation of the radon transforms. In *International Joint Conference on Computer Vision, Imaging and Computer Graphics Theory and Applications (GRAPP)*, 2014.

20. V. Vad, B. Csébfalvi, P. Rautek, and E. Gröller. Towards an unbiased comparison of CC, BCC, and FCC lattices in terms of prealiasing. *Computer Graphics Forum (Proceedings of EuroVis)*, 33(3):81–90, 2014.

21. G. Wang and J. Qi. Direct estimation of kinetic parametric images for dynamic pet. *Theranostics*, 3(10):802–815, 2013.

22. Guobao Wang and Jinyi Qi. An optimization transfer algorithm for nonlinear parametric image reconstruction from dynamic pet data. *Medical Imaging, IEEE Transactions on*, 31(10):1977–1988, Oct 2012.

23. Jianhua Yan, Beata Planeta-Wilson, and R.E. Carson. Direct 4d list mode parametric reconstruction for pet with a novel em algorithm. In *Nuclear Science Symposium Conference Record, 2008. NSS '08. IEEE*, pages 3625–3628, Oct 2008.

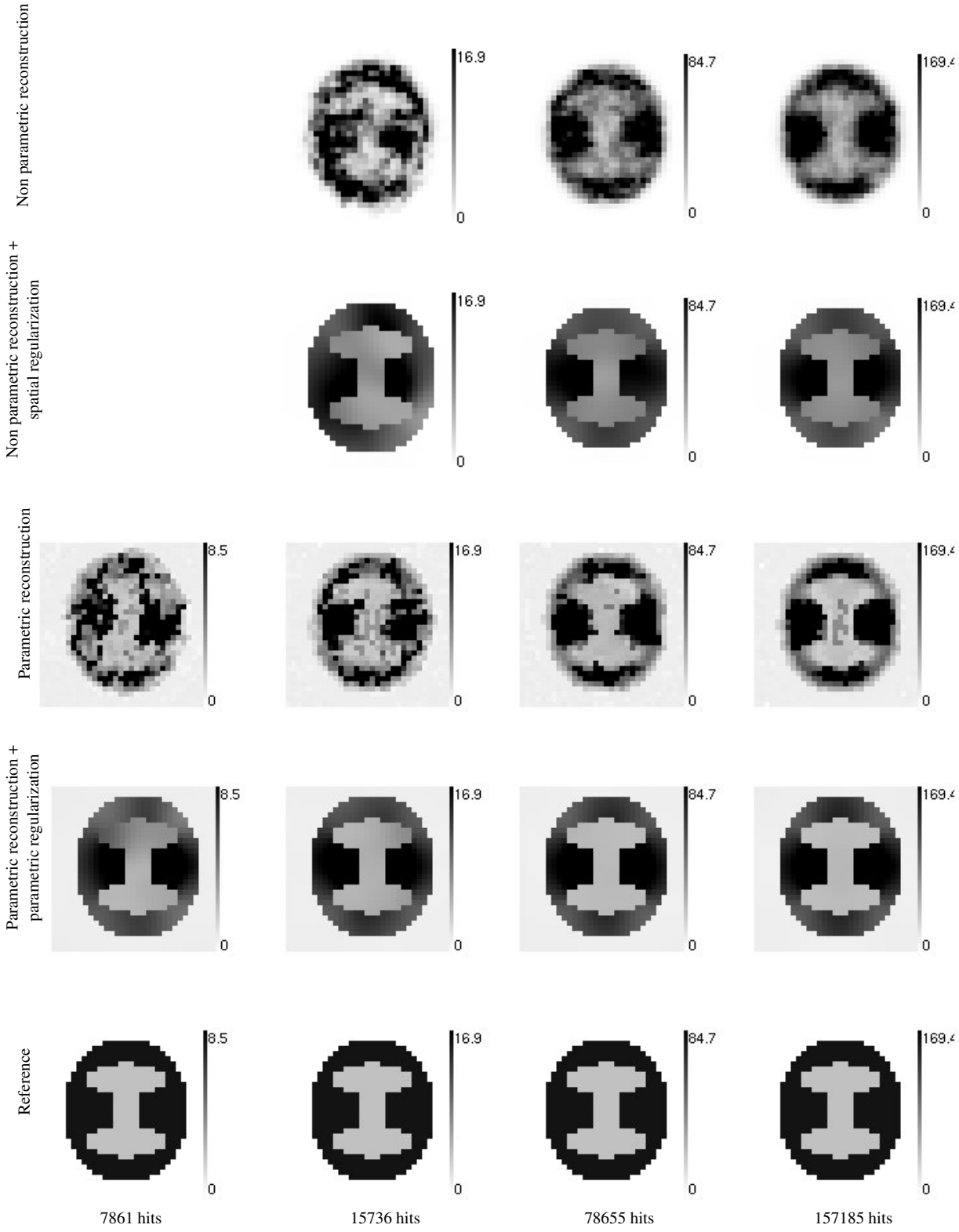

Figure 8: *Examples of reconstructed spatial activity at* $t = 1$.